HAL
open science

On the numerical simulation of multiphase water flows with changes of phase and strong gradients using the Homogeneous Equilibrium Model

Florian de Vuyst, Jean-Michel Ghidaglia, Gérard Le Coq

To cite this version:

Florian de Vuyst, Jean-Michel Ghidaglia, Gérard Le Coq. On the numerical simulation of multiphase water flows with changes of phase and strong gradients using the Homogeneous Equilibrium Model. International Journal on Finite Volumes, 2005, 2 (1), pp.1-36. hal-01123347

HAL Id: hal-01123347

https://hal.science/hal-01123347v1

Submitted on 4 Mar 2015

HAL is a multi-disciplinary open access archive for the deposit and dissemination of scientific research documents, whether they are published or not. The documents may come from teaching and research institutions in France or abroad, or from public or private research centers.

L'archive ouverte pluridisciplinaire **HAL**, est destinée au dépôt et à la diffusion de documents scientifiques de niveau recherche, publiés ou non, émanant des établissements d'enseignement et de recherche français ou étrangers, des laboratoires publics ou privés.

On the numerical simulation of multiphase water flows with changes of phase and strong gradients using the Homogeneous Equilibrium Model

Florian De Vuyst[1,2], Jean-Michel Ghidaglia[2] and Gérard Le Coq[2,3]

November 2004

e-mail: devuyst@mas.ecp.fr, jmg@cmla.ens-cachan.fr, glc@cmla.ens-cachan.fr

Abstract

We introduce a general method based on a variant of the Flux Characteristic method described by Ghidaglia *et al* [22] designed to simulate water-vapour two-phase flows. As an example, we use the three equations Homogeneous Equilibrium model (HEM) with hypotheses of local thermodynamic equilibrium. Our purpose here is to analyze the Finite Volume method when strong gradients of density are present and when some derivatives of quantities like speed of sound strongly vary due to phase transitions. As framework for numerical experiments, we consider a complex flow inside an injector-condenser device. The analysis will lead to a variant of the Flux Characteristic method with regularized matrix-valued sign functions. Other applications like water boiling into a hot channel and a fall of pressure in a crack due to friction will be also considered.

Keywords. - Flux Characteristic Methods, two-phase flows, injector-condenser, phase transition, numerical methods, numerical analysis

AMS Classification. - 35L65, 65M06, 65M12, 65Z05, 76M12, 76N15, 76T10.

[1]Ecole Centrale Paris, Laboratoire Mathématiques Appliquées aux Systèmes, Grande Voie des Vignes 92295 Châtenay-Malabry cedex, France

[2]CMLA, Ecole Normale supérieure de Cachan, CNRS UMR-8536, 61 avenue du Président Wilson, 94235 Cachan cedex, France

[3]Electricité de France, DRD/RNE, 6 quai Watier, 78401 Châtou, France

Contents

1 Introduction and objectives of the present work **3**
1.1 Presentation of the injector-condenser device 3

2 Description and interest of the injector-condenser device **3**
2.1 Compatibility between involved physics and HEM description 4

3 Classical CFD experience versus the two-phase context **5**
3.1 Numerical difficulties 5
3.2 Difficulties due to underlying Physics 6
3.3 Direction of investigation 6

4 Approximation of the equation of state **7**
4.1 Continuity at the phase transitions 8
4.2 Approximation of the convection operator via flux schemes 8

5 A new class of upwind scheme involving regularized sign functions **10**
5.1 First step 10
5.2 Discussion 12
5.3 Second step. Analysis using slopes on both states and flux 13

6 Application to two-phase flows into an injector-condenser **15**

7 Applications on other complex flows **18**
7.1 Boiling water in a hot channel 18
7.2 Fall of pressure in a crack by friction 21

8 Conclusion and future work **22**

9 Appendix A : Derivation of the Homogeneous Equilibrium Model **25**

10 Appendix B : The approximate problem from Homogeneous Equilibrium model **26**

11 Appendix C : equation of state, respect of the first principle of Thermodynamics and entropies **27**
11.1 Examples of partly linear or parabolic laws of state 30
11.2 Computation of constants of the model using water tables 30

1 Introduction and objectives of the present work

1.1 Presentation of the injector-condenser device

Among the two phase flows that are analyzed by thermal-hydraulics, it is known that those with phase changes and phase appearing/desappearing are particularly difficult to simulate numerically. Here, our goal is to perform tools of numerical simulation able to analyze the fluid flow inside an injector-condenser device. It involves complex internal energy exchanges with strong gradients of density and chocking phenomenon (strong condensation). At our knowledge, no satisfactory numerical simulation of the steady flow in the complete injector-condenser has been obtained yet. Let us mention Deberne's works [11] who presented numerical results in agreement with experiments inside the converging part of the nozzle up to the neck.

Our methodology is the following one: we decide to start our numerical investigation using a well-known numerical method used for classical Computational Fluid Dynamics (CFD): we choose the so-called Characteristic Flux Finite Volume (CFFV) method [22],[23] with general numerical flux

$$\Phi(U,V) = \frac{F(U)+F(V)}{2} - \frac{1}{2}\,\mathrm{sgn}(A(U,V))(F(V)-F(U))$$

where sgn denotes the matrix extension of the sign function to diagonalizable matrices and $A(U,V)$ denotes a mean $\mathbb{R}$-diagonalizable matrix depending on states U and V with pure consistency criterion $A(U,U) = D_U F(U)$. That method has the advantage to give a generic upwind process available on any hyperbolic system and does not require the computation of some Roe linearization matrix or shock/rarefaction waves. As starting point, we choose the "simple" Homogeneous Equilibrium Model (HEM) as two-phase model. From numerical experiments where flashing and chocking phenomenons are present, we will attempt to identify a set of numerical difficulties, analyze them for deriving an appropriate scheme, at least in the HEM context. Finally, the part of the real injector-condenser device where the HEM hypotheses are almost valid will be simulated. Some numerical results will be compared to experimental ones for validation and concluding remarks.

2 Description and interest of the injector-condenser device

The injector is a mechanical instrument that is used for drawing along some liquid by using the driving force of another fluid (a gas or fluid). The injector-condenser is a more complex device that has been discovered at the end of the 19th century. Although it has been used for a long time in the industry, the identification of all the physical processes involved is one of the goal of the current research in two-phase flow modelling. This study is motivated by the increasing interest of *Electricité de France* (EDF) for such devices that can be a good alternative to electric compressors in circuits of nuclear power station. An experimental test bed has been implemented at *Institut National de sciences Appliquées* INSA Lyon FRANCE in 1997-99 (see Deberne [11]). It is also used for experimental reference and computational

comparison. Deberne shows the operating principle of the device and gives the operating range in the phase plane (entrance mass flux vs outlet pressure). The INSA team has also identified the good level of description of two-phase flows and has adapted the physical model from the experimental measures.
A simplified presentation of the injector-condensor is given on figure 1. A liquid jet of water

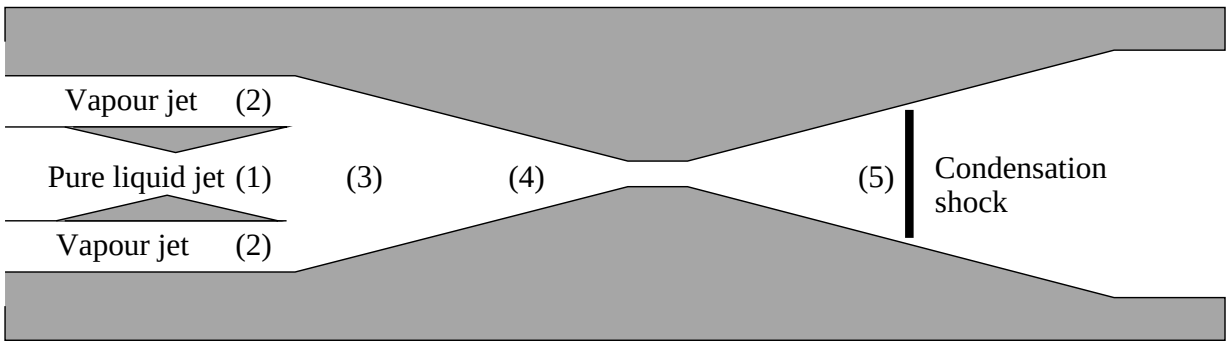

Figure 1: Injector-condenser device

(1) is driven by a faster jet of steam (2). The strong relative velocity between the two phases induces the spraying of liquid that becomes vaporized with a fall of pressure; this is the driving effect of the device. It involves complex processes of mass and energy transfer between the two phases and acts until the total relaxation to local homogeneous velocity and thermodynamic equilibrium conditions. The mixture gradually becomes homogeneous in the admission area (3) and the conditions of thermodynamic equilibrium are observed to be almost reached at the end of the converging part of the nozzle (4). Then, one observes a rapid condensation in the diverging part (5) into pure or almost pure liquid. The energy transfer in the condensation front shows a rise of pressure that can be greater than the inlet pressure. Therefore, the injector-condenser can act as a compressor. The front can be considered as a steady shock wave in the case of the HEM model that assumes an instantaneous relaxation at local thermodynamic equilibrium conditions. The jump Rankine-Hugoniot conditions for a steady shock reflect a flow evolution that passes from an upstream supersonic one to a subsonic state. The flow strongly slows down with a transfer kinetic energy - internal energy. The possible change of phase (from a two-phase mixture to pure liquid) can generate strong discontinuities of the speed of sound, typically from a few meters per second to 1500 ms^{-1} (liquid case), what makes the computation still more difficult.

2.1 Compatibility between involved physics and HEM description

The HEM level of description is not sufficient to simulate all the device because of the presence of mass and heat transfer between phases in the admission area. The simulation of the whole device should in fact involve a “six equations” model. But such a model has inherent difficulties. A hard work of modeling of the exchange terms has to be done in this case;

this matter has been the core of Deberne's Thesis [11]. Note also that the nonconservative products in the system of partial differential equations have no sense when discontinous solutions appear due to nonlinear effects. Both the research team at INSA and engineers from EDF have informed us of their difficulty to capture the condensation phenomenon when using a six equations model with several industrial codes. On the contrary, they have obtained an unexpected effect of reflashing in the diverging part, even though all the quantities correctly evolve from the mixing chamber up to the neck of the nozzle.

3 Classical CFD experience versus the two-phase context

The 30 years old Computational Fluid Dynamic (CFD) experience can enlighten us for good directions of investigation in the two-phase context.

3.1 Numerical difficulties

Since 1975, large efforts of numerical modeling of compressible flows have been developed. Although Reasearch performed important advances for the compressible Euler equations, a "ultimate scheme" (terminology used by van Leer [57]) still does not exist. Actually, the formulation of a large family of efficient conservative schemes (Osher and Solomon [37], kinetic schemes ([6] for recent works on this subject), HUS [9]) intrinsically depend of the structure of continuous or discontinuous waves of approximate Riemann problems, what make them inoperable in the two-phase context because of the too complex structure of Riemann problem solutions. Then the panel of usable methods becomes more tight. The Roe scheme [42] can be used in some cases of multiphase models, but the numerical flux stays not generic and hard work has to be done for the computation of the Roe matrices. More, this work need to be repeated each time the physical model is modified or changed. Today, Roe scheme is still the most employed scheme for two phase applications. Note that recently, Liou extended his AUSM+ scheme to six equations two-phase models [34] and has obtained good results. Today, the relaxation models and relaxation schemes ([10], [26]) are also a major way of research and development. In this paper, we rather use generic methods for model independence purposes. The so-called Characteristic Flux Finite Volume schemes (CFFV, [22],[23]) have the advantage to fulfil this feature. As a starting point, we propose to explore the behavior of CFFV for the injector-condenser problem.

It is interesting to note that the philosophy of both CFD and two-phase worlds can be sometimes divergent. The well-known papers "Towards the ultimate scheme.." written by van Leer ([57] reveal investigation for achieving both stability, robustness and high accuracy. In two phase flows, the sense "Towards the ultimate scheme.." is ambiguous. Indeed, it is known that the core systems of PDEs of two-phase modelling are conditionally hyperbolic (even though strong effort is developed today to find unconditionally hyperbolic systems). Then numerical schemes need to be dissipative enough to produce stable, oscillation free discrete solutions. People often use the Rusanov scheme [45] which is known to be quite dissipative. This is in complete opposition with the usual expectation of accuracy in classical CFD. This is why we will not talk about high order of accuracy in this paper.

3.2 Difficulties due to underlying Physics

Gas dynamics modeling is essentially well-closed, except for particular contexts except when very complex physical phenomena need to be taken into account : chemistry, ionization thermal radiation and plasma coupling for hypersonic flows [35], or compressible turbulence [12], etc. Moreover, equations of state have often a closed form (although possibly implicit) and propagation velocities are well-defined and explicitly determined. Equations are mostly in conservation form. More, a good modeling generally gives entropy-flux pairs that state the well-posedness and the stability of the systems, giving criteria for weak distribution solutions selection. The physical flux is often smooth ($\mathcal{C}^1$) which implies a smooth evolution of derivative-based quantities like the speed of sound. Models do not involve free boundaries (except for fluid-structure interaction problems that are difficult problems).

In two-phase water-vapour flows, there exists some fundamental reasons for which there is still no universally approved closure. One could mention for example the lack of knowledge concerning some microscopic phenomena (*e.g.* nucleation of bubbles at a wall) or the different averaging processes that make loose some properties: hyperbolicity for example. Moreover, it is not always clear how to give a sense to an averaged speed of sound in a mixture of liquid and steam. For the so-called five or six equation models, the equations are written in nonconservation form, and nonconservative products have no sense for discontinuous weak solutions. Finally, for equilibrium models, phase transitions produce a strong jump of speed of sound. That means that the physical flux is not of class $\mathcal{C}^1$, but only Lipschitz continuous. This lack of regularity can be a source of numerical difficulty especially when implicit schemes and fixed point algorithms are used. Moreover, the Homogenous Equilibrium Model (HEM) can lead to aberrant values of Mach-like numbers (up to 100 !). It is also classical in the two-phase world to meet strong (subsonic - supersonic) transition inducing a jump of number of left and right characteristics. For example, for pressure and temperature respectively close to 1 bar and 100 degrees Celcius, the speed of sound can jump from about 1500 ms^{-1} to 5 ms^{-1} in the water. This is the case for a boiling water into a hot channel (see the section of results for simulations). On the other hand, because of the presence of large speed of sound in pure liquid, flow regions of very low mach number are often present. It is then expected to encounter well-known problems of low Mach number (low convergence to steady state and lack of accuracy already observed in classical CFD).

3.3 Direction of investigation

All these difficulties lead us to adopt the following strategy:

(i) begin with the simplest physical model (possibly with no phasic mass or energy transfer),

(ii) work with the smallest number of equations,

(iii) define equations without nonconservative terms,

(iv) study problems with one space variable...

(v) ...while make appear characteristic two-phase behaviours (phase transition, flashing, chocking),

(vi) progressively enrich the model with lowest computational effort and validate Characteristic Fluxes Finite Volume (CFFV) methods.

In this context, the milestone is certainly to insure the three fundamental conservations: mass, momentum and energy. To be more precise, let us consider a quasi-1D flow (see Appendix A) in a pipe (or a nozzle) with variable section σ and constant slip velocity u_r between the two phases. The three aforementioned conservation laws read then as follows :

$$(\rho\sigma)_t + (\rho u\sigma)_x = 0, \tag{1}$$

$$(\rho u\sigma)_t + \left(\sigma\left(\rho u^2 + p + \rho C(1-C){u_r}^2\right)\right)_x = p\sigma_x, \tag{2}$$

$$(\rho E\sigma)_t + \left(\sigma\left(\rho H u + \rho(L + (\frac{1}{2} - C){u_r}^2 + u u_r)C(1-C)u_r\right)\right)_x = 0\,. \tag{3}$$

In these equations, ρ, u and E denote respectively the (mean) density, the velocity and the specific total energy :

$$\rho E = \frac{1}{2}\rho u^2 + \frac{1}{2}\rho C(1-C){u_r}^2 + \rho e\,, \tag{4}$$

p denotes the pressure, C the concentration defined as $\tau = C\tau_v + (1-C)\tau_l$, $H = E + \frac{p}{\rho}$ the specific total enthalpy and L the latent heat.

If the three partial differential equations (1) to (3) are sufficient to describe the evolution of the flow, we have to parametrize the physical state *via* three independent variables. Actually we are going to use two thermodynamic variables and a kinematic one. For the latest, we choose, as it is usually done, the velocity u. Concerning the thermodynamic ones, it will depend on whether we are dealing with a mixture $0 < C < 1$ or a pure fluid $C = 0$ (liquid) or $C = 1$ (vapor).
In the case of a pure fluid, we shall use the temperature T and the pressure p as independent variables, *i.e.* we consider all the quantities as functions of (p, T, u). While in the case of a mixture, we shall use the temperature T and the concentration C as independent variables, *i.e.* we express all the quantities as functions of (C, T, u).

4 Approximation of the equation of state

Starting with a numerical value of the set of three conservative variables $v = (\rho\sigma, \rho u\sigma, \rho E\sigma)$, we want to compute the corresponding value of the flux $f(v)$ given by formula (13). This requires the computation of the thermodynamic variables. In the case where $u_r = 0$, as we know that v immediately enables the computation of ρ and e, and then that one has to find either T and C or p and T depending on whether we are dealing with a mixture or not. This is an inverse problem which has to be solved numerically by using an iterative method (we shall use Newton's one). At each iteration, one has to compute thermodynamic variables or coefficients by using water tables. This can be very costly in terms of CPU time and therefore, we suggest a proper linearization of such tables which leads to a more efficient

method without loosing the physical meaning of the equations of state (see Appendix C for the complete construction).

4.1 Continuity at the phase transitions

We denote by ρ_k, $\tau_k \equiv 1/\rho_k$, h_k, $e_k \equiv h_k - p_k\tau_k$ and s_k, the density, the specific volume, the specific enthalpy, the specific internal energy and the specific entropy of the fluid, the index k being either ℓ for the liquid or v for the vapor.
Suppose that the laws $\tau_\ell(p,T)$, $h_\ell(p,T)$, $\tau_v(p,T)$ and $h_v(p,T)$ are known. In the two-phase mixture, both the liquid and the vapour phases change at conditions of saturation. In that case, the pressure is linked to the temperature by the law of pressure of saturation p_s :

$$p \;=\; p_s(T) \tag{5}$$

This function is expected to be continuously differentiable and strictly monotonous, so that we can notably invert it to get the temperature of saturation T_s as function of the pressure $T \;=\; T_s(p) \;=\; (p_s)^{-1}(p)$. So we can respectively define the specific volume and enthalpy of saturation by

$$\tau_{k;s}(T) \;=\; \tau_k(p_s(T),T), \tag{6}$$
$$h_{k;s}(T) \;=\; h_k(p_s(T),T) \tag{7}$$

where the subscript k equals to l or v. Finally, we define some average quantities τ and h to define the mixture. The concentration C, $0 \le C \le 1$ infers on the extensive variables τ and h. The pair (C,T) is defined as the unique solution in $[0,1]\times]0,+\infty[$ of

$$\tau \;=\; C\;\tau_{v;s}(T) + (1-C)\tau_{l;s}(T), \tag{8}$$

$$h \;=\; C\;h_{v;s}(T) + (1-C)h_{l;s}(T). \tag{9}$$

Consequently, variables C and T play the role of free thermodynamic variables in the mixture.

4.2 Approximation of the convection operator via flux schemes

The system (1) to (3) can be written as :

$$\frac{\partial U}{\partial t} + \frac{\partial F(U)}{\partial x} = S(U)\,, \tag{10}$$

with

$$U = (\rho\sigma, \rho u\sigma, \rho E\sigma)\,, \tag{11}$$
$$S(U) = (0, p\sigma_x, 0)\,, \tag{12}$$
$$F(U) = (F_1(U), F_2(U), F_3(U))\,, \tag{13}$$
$$F_1(U) = \rho u\sigma,$$
$$F_2(U) = \left(\rho u^2 + p + \rho C(1-C){u_r}^2\right)\sigma\,,$$
$$F_3(U) = \left(\rho H u + \rho(L + (\frac{1}{2} - C){u_r}^2 + u u_r)C(1-C)u_r\right)\sigma.$$

We denote by $A(U)$ the Jacobian matrix $\frac{\partial F(U)}{\partial U}$ and we assume that the three characteristic velocities are distinct *i.e.* $\Delta > 0$. Hence (10) is *regularly hyperbolic* that is to say: for every U there exists a smooth basis $(r_1(U), r_2(U), r_3(U))$ of $\mathbb{R}^3$ made of eigenvectors of $A(U)$: $\exists \lambda_k(U) \in \mathbb{R}$ such that $A(U)r_k(U) = \lambda_k(U)r_k(U)$. It is then possible to construct a $(l_1(U), l_2(U), l_3(U))$ such that ${}^tA(U)l_k(U) = \lambda_k(U)l_k(U)$ and $l_k(U) \cdot r_p(U) = \delta_{k,p}$.
Let $\mathbb{R} = \cup_{j\in\mathbb{Z}}[x_{j-1/2}, x_{j+1/2}]$ be a one dimensional mesh. Our goal is to discretize (10) by a finite volume method. We look for an approximation U_j^n of $U(x_j, t_n)$ defined by

$$\frac{1}{\Delta x_j \Delta t_n} \int_{x_{j-1/2}}^{x_{j+1/2}} \int_{t_n}^{t_{n+1}} U(x,t)\, dx\, dt,$$

with $\Delta x_j \equiv x_{j+1/2} - x_{j-1/2}$, $\Delta t_n \equiv t_{n+1} - t_n$ (we also have $\mathbb{R}_+ = \cup_{n\in\mathbb{N}}[t_n, t_{n+1}]$). The discretization of (10) according to the implicit Characteristic Flux Method (Ghidaglia, Kumbaro and Le Coq [22],[23]) reads as :

$$U_j^{n+1} = U_j^n - \frac{\Delta t_n}{\Delta x_j}\left(F_{j+1/2}^{n+1} - F_{j-1/2}^{n+1}\right) \; + \; \Delta t_n\, S_j^{n+1}\,, \tag{14}$$

About the important question of the numerical treatment of the source terms (computation of S_j^{n+1}), we use the same upwind strategy as exposed in Alouges *et al* [1]. The implicit characteristic flux $F_{j+1/2}^{n+1}$ is obtained by the following formula

$$F_{j+1/2}^{n+1} = G_{j+1/2}^{CF}(U_j^n, U_{j+1}^n; F(U_j^{n+1}), F(U_{j+1}^{n+1}))\,, \tag{15}$$

and

$$G_{j+1/2}^{CF}(U,V;F,G) \equiv \frac{F+G}{2} - B(\mu_{j+1/2}; U, V)\frac{G-F}{2}\,, \tag{16}$$

where $\mu_{j+1/2}$ is a mean value between the two states U and V which depends also on Δx_j and Δx_{j+1} and $B(\mu; U, V)$ is the sign of the matrix $A(\mu)$:

$$B(\mu; U, V)\Phi = \sum_{k=1}^{3} \mathrm{sgn}(\lambda_k(\mu))(l_k(\mu)\cdot\Phi)r_k(\mu)\,. \tag{17}$$

In this last formula, since $\mathrm{sgn}(\lambda) = -1$ or 1, this numerical flux can be irregular in some particularly stiff instances. This feature occurs for example at phase transitions between the pure liquid and the two-phase mixture. Because the eigenvalues are computed using an averaged state μ, we have to decide whether this mean state is liquid or corresponds to a mixture. In both cases, one favours one state rather than one another. More, because the scheme is implicit, an iterative fixed point algorithm like Newton's method is used to solve the resulting nonlinear system of equations to solve at each time step. Because the flux is not differentiable at transition, numerical spurious oscillations (sensible on pressure profile) appear and make the computation unstable.
To provide some regularity on the numerical flux, we propose in the next section a smoother family of numerical fluxes that does not strictly fall into the family of characteristic fluxes, but can approach them as close as we want *via* a regularization parameter ϵ. This is equivalent

to a regularization process of the *sign* functions. The truncated numerical dissipation due to regularization needs to be compensated by an additional term of the form

$$-Q_\epsilon(\mu_{j+1/2}; U, V)\,\frac{V-U}{2}$$

for a particular dissipation matrix $Q_\epsilon \geq 0$ that vanishes when $\epsilon \to 0$.

5 A new class of upwind scheme involving regularized sign functions

5.1 First step

We are looking for the "best" local interpolation inside two adjacent cells I and J of respective constant state U and V. For the sake of simplicity, suppose that $|I| = |J| = h$. Given a first order numerical flux, the interpolation must respect the upwinding feature. We still work on a hyperbolic system of conservation laws

$$\partial_t U + \partial_x F(U) = 0,\ U, F(U) \in \mathbb{R}^p$$

The interpolation is supposed piecewise linear per cell with possible discontinuity at interface. We then define two interpolation states at interface:

$$\tilde{U} \ = \ U + \frac{1}{2} S_U (V-U),\ \tilde{V} \ = \ V - \frac{1}{2} S_V (V-U), \tag{18}$$

where S_U, $S_V \in \mathcal{M}_p(\mathbb{R})$. The construction of such matrices is detailed later. At the moment, let $A(U,V)$ be a matrix that satisfies both consistency and decomposition conditions:

$$\begin{array}{l} A(U,V) \text{ is diagonalizable in } \mathbb{R}, \\ A(U,U) \ = \ D_U F(U). \end{array} \tag{19}$$

We denote by $(\lambda_k)_{k=1,p}$ the eigenvalues of $A(U,V)$ and R the matrix of right eigenvectors arranged in column, so we have the decomposition

$$A \ = \ R\,\mathrm{diag}\,(\lambda_k)\,R^{-1}.$$

The matrices S_U and S_V can be more precisely detailed. We equip these matrices of family of slope parameters $(s_{k;U})_{k=1,p}$ and $(s_{k;V})_{k=1,p}$ estimated in the basis of eigenvectors, that means

$$S_U \ = \ R\,\mathrm{diag}\,(s_{k;U})\,R^{-1},\ S_V \ = \ R\,\mathrm{diag}\,(s_{k;V})\,R^{-1}. \tag{20}$$

Finally, let $q \in [0,1]$. We consider a family of upwind numerical fluxes $(q, s_{k;U}, s_{k;V})$ of the form

$$\Phi(U,V) \ = \ \frac{F(\tilde{U}) + F(\tilde{V})}{2} - \frac{1}{2}\,q\,|A(U,V)|\,(\tilde{V} - \tilde{U}).$$

We are going to characterize necessary and sufficient conditions on $(q, s_{k;U}, s_{k;V})$ to have a smooth (locally Lipschitz continuous) and upwind numerical flux.

Monotonicity criteria.

Proposition 1 *The condition of monotony property for the local interpolation is*

$$0 \;\leq\; s_{k;U} \;\leq\; 2, \quad 0 \;\leq\; s_{k;V} \;\leq\; 2. \tag{21}$$

Remark that the case $S_U = S_V = I$ gives a second order interpolation.

Upwinding and continuity criteria

Proposition 2 *1. The conditions for upwind process are*

$$-\,q\,\frac{s_{k;U}+s_{k;V}}{2} \;+\; \mathrm{sgn}(\lambda_k)\,\frac{s_{k;V}-s_{k;U}}{2} \geq\; 1-q \qquad \forall k \in \{1...p\}, \tag{22}$$

2. The only admissible value of q for continuous coefficients α_k at sonic points $\lambda_k = 0$ is $q = 1$.

Proof. We expose the proof in the linear case $F(U) = A\,U$ for constant matrix A. We write the explicit difference scheme of initial state V in the left half of the cell J at the right of the interface (I, J):

$$\begin{aligned} V^{n+1} \;&=\; V - 2\mu_n \left\{ AV - \frac{1}{2}A\,(V+U) + \frac{1}{2}R\,\mathrm{diag}\left(\lambda_k\,\frac{s_{k;U}+s_{k;V}}{2}\right) R^{-1}(V-U) \right. \\ &+\; \left. \frac{1}{2}\,q\,|A|\,R\,\mathrm{diag}\left(1-\frac{s_{k;U}+s_{k;V}}{2}\right) R^{-1}(V-U) \right\}, \end{aligned}$$

where $\mu_n = \Delta t_n/h$. The expression can be written again

$$V^{n+1} \;=\; V - 2\mu^n\; R\,\mathrm{diag}\left(\frac{1}{2}\lambda_k + \frac{1}{2}q\,|\lambda_k|\,(1-\frac{s_{k;U}+s_{k;V}}{2}) + \frac{1}{2}\lambda_k\frac{s_{k;V}-s_{k;U}}{2}\right) R^{-1}\;(V-U).$$

The scheme is expected to be upwind. We want to only capture the positive propagation velocities in the half cell, so that we are looking for coefficients such that

$$\frac{1}{2}\lambda_k + \frac{1}{2}q\,|\lambda_k|\,(1-\frac{s_{k;U}+s_{k;V}}{2}) + \frac{1}{2}\lambda_k\frac{s_{k;V}-s_{k;U}}{2} \;\geq\; 0$$

is true for all k. This gives

$$\frac{1-q}{2}\,s_{k;V} \;-\; \frac{1+q}{2}\,s_{k;U} \geq\; -1-q$$

for $\lambda_k \geq 0$ and

$$-\frac{1-q}{2}\,s_{k;U} \;+\; \frac{1+q}{2}\,s_{k;V} \leq -1+q$$

for $\lambda_k \leq 0$. In the same way, the scheme in the left half cell of initial state U gives

$$U^{n+1} \;=\; U - 2\mu^n\; R\,\mathrm{diag}\left(-\frac{1}{2}\lambda_k + \frac{1}{2}q\,|\lambda_k|\,(1-\frac{s_{k;U}+s_{k;V}}{2}) + \frac{1}{2}\lambda_k\frac{s_{k;V}-s_{k;U}}{2}\right) R^{-1}\;(V-U)$$

with conditions

$$\frac{1-q}{2}\,s_{k;V} \;-\; \frac{1+q}{2}\,s_{k;V} \geq\; 1-q$$

for $\lambda_k \geq 0$ and

$$-\frac{1-q}{2}\, s_{k;U} \;+\; \frac{1+q}{2}\, s_{k;V} \leq 1+q$$

for $\lambda_k \leq 0$. Secondly, we are looking conditions on q to have continuity on coefficients at $\lambda_k = 0$. By difference one gets

$$q\,(s_{k;U} + s_{k;V}) \;=\; 2(q-1) \;\; \forall k.$$

This is only possible for $q = 1$. In that case, if $\lambda_k = 0$, we find $s_{k;U} = s_{k;V} = 0$.

Corollary 1 *In the case $q = 1$, the admissible values for $s_{k;U}$ ad $s_{k;V}$ are*

$$\begin{aligned}
&\textit{If } \lambda_k > 0, \;\; \textit{then } s_{k;U} = 0, \;\; 0 \leq s_{k;V} \leq 2,\\
&\textit{if } \lambda_k < 0, \;\; \textit{then } 0 \leq s_{k;U} \leq 2, \;\; s_{k;V} = 0,\\
&\textit{if } \lambda_k = 0, \;\; \textit{then } s_{k;U} = s_{k;V} = 0.
\end{aligned}$$

5.2 Discussion

There exists some large degrees of freedom for the design of coefficients $s_{k;U}$ $s_{k;V}$ (see as functions of eigenvalues λ_k).
The idea here is to choose slope coefficients that are simple to calculate and give good properties. Let us first recall the expression of the numerical flux for $q = 1$:

$$\begin{aligned}
\Phi(U,V) \;&=\; \frac{1}{2}\left\{F(U + \frac{1}{2}S_U(V-U)) + F(V - \frac{1}{2}S_V(V-U))\right\}\\
&\quad - \frac{1}{2}\left(I - \frac{S_U + S_V}{2}\right)|A(U,V)|\,(V-U).
\end{aligned}$$

1. First, states U and V play the same role. The symmetry invite us to choose

$$s_{k;V}(\lambda) \;=\; s_{k;U}(-\lambda).$$

2. There is a priori no reason to distinguish the different fields of the system, so we propose

$$s_{k;U}(\lambda) \;=\; \chi(\lambda)$$

independent of k.
3. Function χ is supposed to be at least Lipschitz continuous. For numerical purposes, it is reasonable to design these functions as piecewise smooth.
4. The shape of the numerical flux shows a flux term added by a viscous term. Again for numerical reasons like accuracy requirement, it is natural to try to put the maximum information into the flux terms. Suppose that all the waves produced by the interaction of the two states are positive. Then necessary, $s_{k;U} = 0 \;\forall k$. Consequently, the choice $s_{k;V} = 2 \;\forall k$ which is admissible makes the viscous term falling down to zero. On the other hand ($s_{k;V} = 2 \;\forall k$), we get

$$\Phi(U,V) \;=\; F(U). \tag{23}$$

This is exactly the expected flux which is also the Godunov flux known to satisfy discrete entropy inequalities. By this construction, this family falls into the class of upwind difference schemes this the definition given by Harten, Lax and van Leer [30].
Of course, because of the continuity constraints at $\lambda = 0$ with $s_{k;U} = 0$, this property cannot be true for values λ_k belonging to a "small" interval $[0, \epsilon]$, $\epsilon > 0$. Up to a parameter, we can choose $\chi(\lambda) = 2\ \forall \lambda \in [\epsilon, +\infty[$. Parameter ϵ could be chosen according to the minimum distance between two consecutive waves for example. For simplicity, we suppose here that all the characteristic fields are simple, otherwise we should group all the linearly degenerate fields with same eigenvalue and the construction still holds. We resume the previous construction and remarks by the following result:

Proposition 3 *From any admissible states U and V, we define a mean diagonalizable matrix $A(U, V)$ that respects the consistency condition $A(U, U) = A(U)$. Let $\lambda_k(U, V)$ be the kth eigenvalue of $A(U, V)$ and ϵ a positive real number such that*

$$\epsilon \ < \ \min_k |\lambda_{k+1}(U, V) - \lambda_k(U, V)| \,. \tag{24}$$

Let $\chi_\epsilon : \mathbb{R} \to [0, 2]$ be a locally Lipschitz continuous function such that

$$\begin{array}{rcl} \chi(x) & = & 0 \quad \forall x \geq 0, \\ \chi(x) & = & 2 \quad \forall x \leq \epsilon. \end{array} \tag{25}$$

Then the following numerical scheme with numerical flux $\Phi(U, V)$ equal to

$$\begin{aligned} \frac{1}{2} \Big\{ F(U + \frac{1}{2} R \operatorname{diag}(\chi_\epsilon(\lambda_k)) R^{-1}(V - U)) + F(V - \frac{1}{2} R \operatorname{diag}(\chi_\epsilon(-\lambda_k)) R^{-1}(V - U)) \Big\} \\ - \frac{1}{2} \left(I - R \operatorname{diag} \left(\frac{\chi_\epsilon(\lambda_k) + \chi_\epsilon(-\lambda_k)}{2} \right) R^{-1} \right) |A(U, V)| \, (V - U). \end{aligned} \tag{26}$$

leads to an upwind scheme in the sense of Harten, Lax and van Leer with Lipschitz continuous flux. The stability criterion is given by

$$\mu_n \ \max_{j \in \mathbb{Z}} \max_k |\lambda_k(A(U_j, U_{j+1}))| < 1.$$

Let us remark that the flux cannot be read under a usual viscous form and that the interpolated states $U + \frac{1}{2} R \operatorname{diag}(\chi_\epsilon(\lambda_k)) R^{-1}(V - U)$ can become not be admissible (negative density, negative energy for example). This motivates us to introduce interpolations that are now applied to the fluxes.

5.3 Second step. Analysis using slopes on both states and flux

The same analysis can be performed combining both slopes on states and flux. We here more define two interpolated flux $\tilde{F}_U$ and $\tilde{F}_V$ with expressions

$$\tilde{F}_U \ = \ F(U) + \frac{1}{2} S_U \left(F(V) - F(U) \right), \ \tilde{F}_V \ = \ F(V) - \frac{1}{2} S_V \left(F(V) - F(U) \right), \tag{27}$$

sharing the same slope coefficients than the states. We are looking for a numerical flux of the form

$$\Phi(U,V) \;=\; \frac{\tilde{F}_U+\tilde{F}_V}{2} - \frac{1}{2}\,q\;|A(U,V)|\;(\tilde{V}-\tilde{U}).$$

For $q=1$, the numerical flux has the following viscous form

$$\Phi(U,V) \;=\; \frac{F_U+F_V}{2} \;-\; \frac{1}{2}\frac{S_V-S_U}{2}\,(F(V)-F(U)) \;-\; \frac{1}{2}\left(\mathsf{I}-\frac{S_U+S_V}{2}\right)\,|A(U,V)|\;(V-U). \tag{28}$$

It is written in viscous form. More, its script is close to those of characteristic flux schemes introduced by Ghidaglia, Kumbaro and Le Coq [22],[23]. If functions $s_{k;U}$ and $s_{k;V}$ are built from a function χ_ϵ as discussed before, it is clear to see that the odd function

$$\frac{s_{k;V}-s_{k;U}}{2} \;=\; \frac{\chi_\epsilon(-\lambda_k)-\chi_\epsilon(\lambda_k)}{2}$$

with values in $[-1,1]$ plays the role of a regularized sign function, whereas the compactly bounded support even function

$$1-\frac{s_{k;V}+s_{k;U}}{2} \;=\; 1-\frac{\chi_\epsilon(-\lambda_k)+\chi_\epsilon(\lambda_k)}{2}$$

with values in $[0,1]$ provides the missing numerical dissipation for strict upwinding and stability. We can finally resume:

Proposition 4 *Under the same hypotheses than Proposition 1, the difference scheme with numerical flux*

$$\Phi(U,V) = \frac{F_U+F_V}{2} \;-\; \frac{1}{2}\,R\,\mathrm{diag}\,(\sigma_\epsilon(\lambda_k))\,R^{-1}(F(V)-F(U)) - \;\frac{1}{2}\,R\,\mathrm{diag}\,(\hbar_\epsilon(\lambda_k))\,R^{-1}(V-U), \tag{29}$$

with

$$\sigma_\epsilon(\lambda) = \frac{\chi_\epsilon(-\lambda_k)-\chi_\epsilon(\lambda_k)}{2}, \quad \hbar_\epsilon(\lambda) = 1-\frac{\chi_\epsilon(\lambda_k)+\chi_\epsilon(-\lambda_k)}{2}$$

has the same properties of smoothness and upwinding. The limit case $\epsilon\to 0$ gives the family of characteristic flux schemes.

Example of numerical flux The simplest Lipschitz continuous flux is built using the piecewise linear function χ_ϵ

$$\chi_\epsilon(\lambda) = \begin{cases} 2 \text{ if } \lambda \le -\epsilon, \\ -\frac{2\lambda}{\epsilon} \text{ if } -\epsilon < \lambda \le 0, \\ 0 \text{ otherwise.} \end{cases} \tag{30}$$

Proposition 5 *For the choice (30),*

$$\sigma_\epsilon(\lambda) \;=\; \begin{cases} \mathrm{sgn}(\lambda) \;\textit{if}\; |\frac{\lambda}{\epsilon}| \ge 1, \\ \frac{\lambda}{\epsilon} \;\textit{otherwise}, \end{cases} \qquad \hbar_\epsilon(\lambda) \;=\; \begin{cases} 1-\left|\frac{\lambda}{\epsilon}\right| \;\textit{if}\; |\frac{\lambda}{\epsilon}| \le 1, \\ 0 \;\textit{otherwise.} \end{cases} \tag{31}$$

or again under a condensed form

$$\sigma_\epsilon(\lambda) = \min\left(1, \left|\frac{\lambda}{\epsilon}\right|\right) \operatorname{sgn}(\frac{\lambda}{\epsilon}),\ \hbar_\epsilon(\lambda) = \max\left(0, 1 - \left|\frac{\lambda}{\epsilon}\right|\right)$$

Function σ_ϵ plays the role of a regularized sign function.

Another interesting feature of the last construction is that the resulting scheme preserves stationary contact discontinuities provided additional hypotheses on $A(U,V)$ that are easy to fulfil. So it provides strong accuracy for slowly moving linear waves.

Proposition 6 *Suppose more that $A(U,V)$ preserves the kth Riemann invariant λ_k for two states U and V separated by a k-contact discontinuity, that means*

$$\lambda_k(A(U,V)) = \lambda_k(A(U)) = \lambda_k(A(V)),\ k \in LD(F),$$

where $LD(F)$ is the set of indices $k \in \{1, ..., p\}$ of linearly degenerate fields for flux F. Then the difference scheme of numerical flux (29) perfectly preserves stationary contact discontinuities.

Proof. Suppose that $F(U) = F(V)$, $U \neq V$ with $\lambda_k(A(U) = \lambda_k(A(V)) = \lambda_k(A(U,V)) = 0$. So the first dissipation term in (29) is zero. Then the kth eigenvalue of diagonal matrix $\operatorname{diag}(\hbar_\epsilon(\lambda_l)|\lambda_l|)$ is zero. Otherwise, because ϵ does not exceed the distance between two eigenvalues (by hypothesis (24)) and because function $\hbar_\epsilon$ is compactly supported on the interval $[-\epsilon, \epsilon]$, then $\hbar_\epsilon(\lambda_l) = 0$ for all $l \neq k$.

This numerical flux can be straitforwardly extended to multidimensional problems using for example the property of invariance by rotation of the equations.

6 Application to two-phase flows into an injector-condenser

We present two examples of injector-condenser configuration. The first one is a "6 bar" example and has been built to validate the whole flux scheme method [22]. The model constants given by table 2 of Appendic C are used. The second one corresponds to a real case extracted from conditions of experiment of the INSA test bed. In this case, data from table 1 of Appendix C are used. Because we cannot simulate the whole device, we have extracted data from experiments at the position of converging nozzle where the homogeneous equilibirum hypothesis is almost verified. Because the flow is supersonic in this area, this can define the entrance of our computational domain and we can use measured data as inlet boundary conditions. In both cases, the source terms are $S_2(v) = p\frac{\partial\sigma}{\partial x}$ that models the influence of the geometry and $S_3(v) = 0$ (no heat flux).

Six bar injector-condenser test case. The nozzle is 1 meter long. We use 150 computational points with a uniform space step. The section σ is defined as

$$\sigma(x) \ = \ \begin{cases} 1 - 0.015\left(1 - w^2(3-2w) + 15w^2(1-w)^2\right) \text{ if } 0 \leq w \leq 1, \\ 1 \text{ otherwise,} \end{cases}$$

where $w = x/0.9$. The process to capture an operating mode at imposed outlet pressure ($p_s = 6.8$ bar) is similar to the experimental one. First, we impose an outflow pressure lower than p_s, that is to say 6 bar. The entrance mass flux $\rho u \sigma$ will be chosen small enough in order to get first a whole subsonic flow. The field is initialized with a two-phase mixture at uniform pressure $p = 6$ bar and a concentration $C = 10^{-2}$. Because the flow is subsonic at the entrance, we have to impose an additional constraint, namely on the specific enthalpy h compatible with the constraints $p = 6$ bar and $C = 10^{-2}$. Secondly, we successively increase the values of inflow mass flux and outlet pressure in order to produce a supersonic region, coming with the condensation shock and to stabilize the shock in the computational domain. At fixed outlet pressure, increasing the inlet mass flux shifts the condensation to the right. At fixed inlet mass flux, increasing the outlet pressure results in shifting the shock to the left. Finally, at the end of the computation, the inflow mass flux is equal to $\rho u \sigma = 3700$ (in SI unit). On figure 2, we summarize the strategy of operation. On figure 3, we show

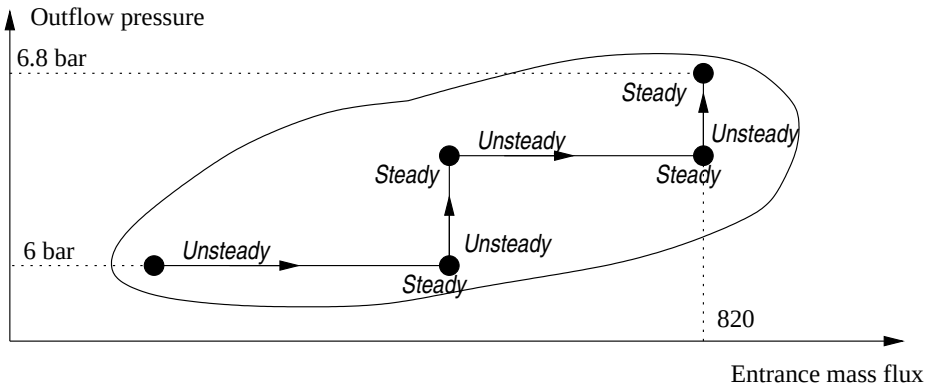

Figure 2: Strategy of computation at fixed outflow pressure 6.8 bar

the nozzle section profile and the numerical steady solutions obtained at $p_s = 6.8$ bar. On a Mollier diagram, it can be verified that all the thermodynamic variables evolve correctly, which validates our approximation on the equations of state.
Then, the main difficulty during the computation is linked to the points of phase transition, where the physical flux is not differentiable (only Lipschitz continuous). The numerical consequence of this weak regularity is the creation of large oscillations during the fixed point algorithm used to solve the nonlinear implicit method. Sometimes it happens that the code breaks down when too large Courant numbers are used. For the moment, our only alternative is to drastically reduce the CFL number to one during transitions. Without phase transition, large Courant numbers up to 50000 can be used.

INSA test bed simulation. This numerical test case dimensionized on the experimental test bed of INSA Lyon. We use the geometry of the INSA nozzle and same generating boundary conditions. Because we cannot describe the transfer effects in the admission chamber with our model, our computational domain only begins around the middle of the converging part of the nozzle. The computational observation domain is 0.320 m long for $0.180 < x < 0.5$

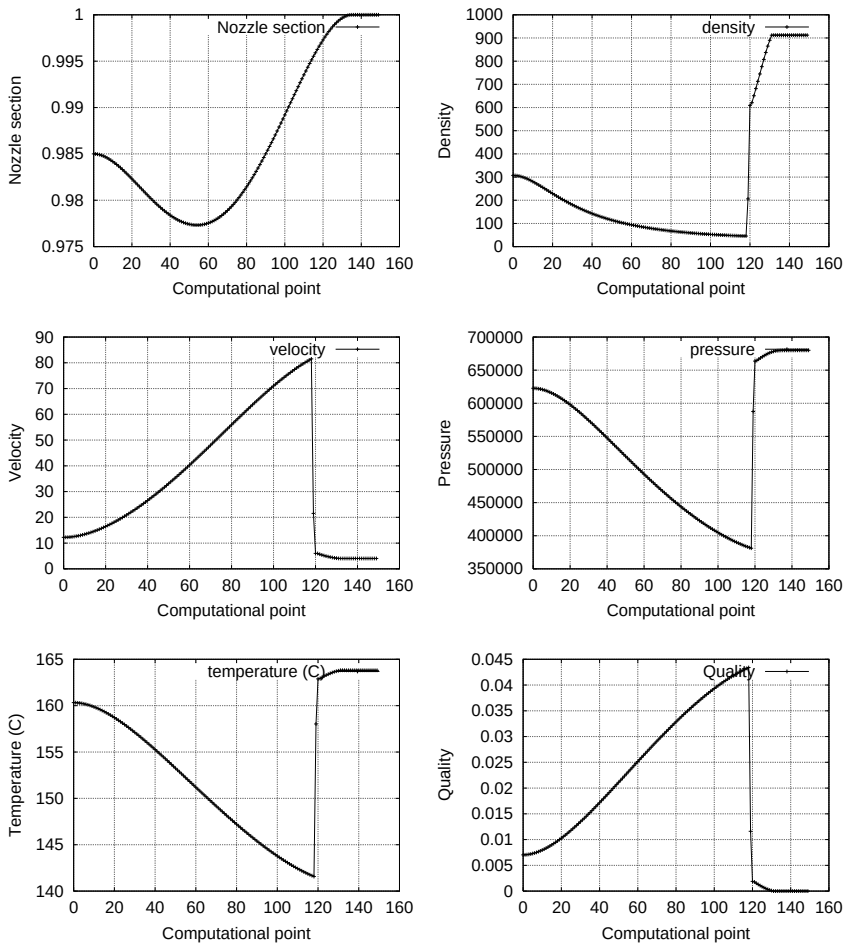

Figure 3: Profiles of steady solutions for the 6 bar injector-condenser test case

with section σ given by

$$\sigma(x) \;=\; \begin{cases} 0.06 + \frac{0.075-0.06}{0.307-0.015}(x-0.015) \text{ if } 0.180 < x < 0.307, \\ 0.0075 \text{ if } 0.307 \leq x < 0.322, \\ 0.0075 + \frac{0.045-0.075}{0.500-0.322} \text{ if } 0.322 \leq x < 0.500. \end{cases}$$

At the left entrance boundary, the flow is supersonic so that we have to impose three conditions. Deberne has communicated us the measured data at this location, which corresponds to a two-phase mixture state with almost homogeneous velocity and thermodynamic equilibrium conditions (in SI unit) :

$$\rho \;=\; 127.06228, \quad u \;=\; 6, \quad h \;=\; 355380.272.$$

Using the same strategy as described above, we have tried to identify a large range of operation for this injector-condenser. We have been again confronted to the problem of robustness due to the lack of regularity of the flux at transition points which has limited our exploration of the operating range of the device. On figure 4, we present results obtained for an outlet pressure increased to about 0.25 bar.

7 Applications on other complex flows

7.1 Boiling water in a hot channel

The problem consists in heating some water in a channel of constant section. For that purpose, we add a source term of exchange by heat flux between the wall and the water. The vector source term is independent of the state, equal to $S(v) = {}^t(0, 0, \Phi(x,t))$ where then function Φ is described below. We suppose a slight nonequilibrium on velocity with constant relative velocity equal to $u_r = 0.1$. We decide that at the inflow, the fluid is expected to be made of pure undersaturated liquid. The heat flux Φ is calculated in such a way that the fluid at the outflow is made of dry oversaturated vapour. In that way, we should observe at the steady flow three regions of fluid of different nature separated by two points of phase transition. We do not know a priori the position of the phase transitions so that this consists in solving a free boundary problem. This academic problem let us verify the capacity of the method to correctly select the proper equations of state according to the nature of the fluid. Channel is 7 meter long. We choose $\sigma = 1$ and use 30 computational points with a constant space step. The flow is aimed at staying subsonic and evolving near 1 bar. Because of this last requirement, we use the constants of the model given at table 1. For the boundary conditions, we impose at the entrance the mass flux $\rho u = 1$ and the specific enthalpy which is compatible with a liquid of pressure 1 bar and temperature 50 degrees Celcius. At the outlet, we impose a pressure equal to 1 bar. The initial flow is a uniform liquid flow with values $p = 1$ bar, $T = 50$ C and $\rho u = 1$. For the heat flux function, we choose

$$\Phi(x,t) \;=\; \begin{cases} \Phi_{max} \;\min\left(\frac{t}{5000}, 1\right) \;\left(x + x^2(1-x)\right) \quad \text{if } 0 < x < 1 \\ 450000 \;\min\left(\frac{t}{5000}, 1\right) \text{ if } 1 < x < 3.5 \\ + \text{ symmetry for } 3.5 < x < 7\,. \end{cases}$$

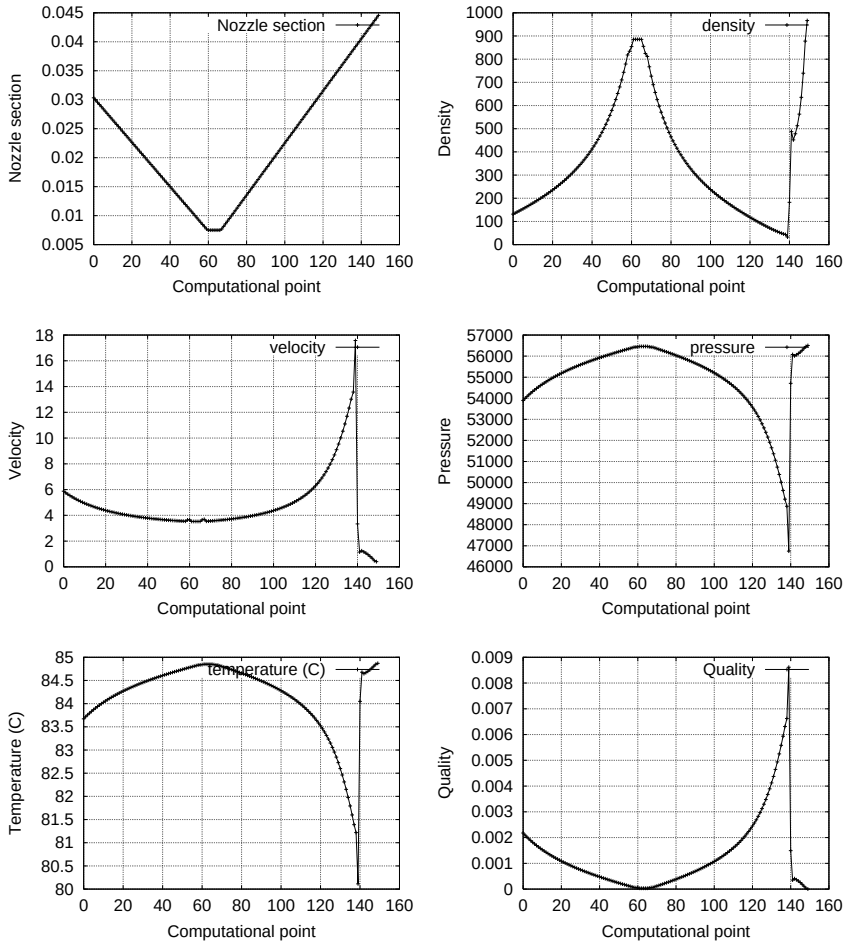

Figure 4: Profiles of steady solutions for the INSA injector-condenser device

The maximum value “450000” has been set so that the fluid is made of dry vapour at the outlet once the steady state is reached.
The implicit method enables us to use CFL numbers up to 50000, leading to small time of computation of order a few minutes on Sun Ultra platforms. But we acknowledge problems of robustness at the liquid - mixture phase transition during the unsteady flow even when using the flux correction discussed in section 4.2. That constrained us to strongly reduce the CFL number (down to one) during the phase of stabilization of the phase transition points. On figure 5, we present numerical results for the steady flow. They are in very good agreement with the theoretical solution which can be exhibited in one space dimension by integrating the ODEs. In particular, we have verified that, for $u_r = 0$, the concentration C linearly varies from zero to one in the two-phase mixture region. We observe that the pressure stays in the vicinity of 1 bar (saturation pressure).

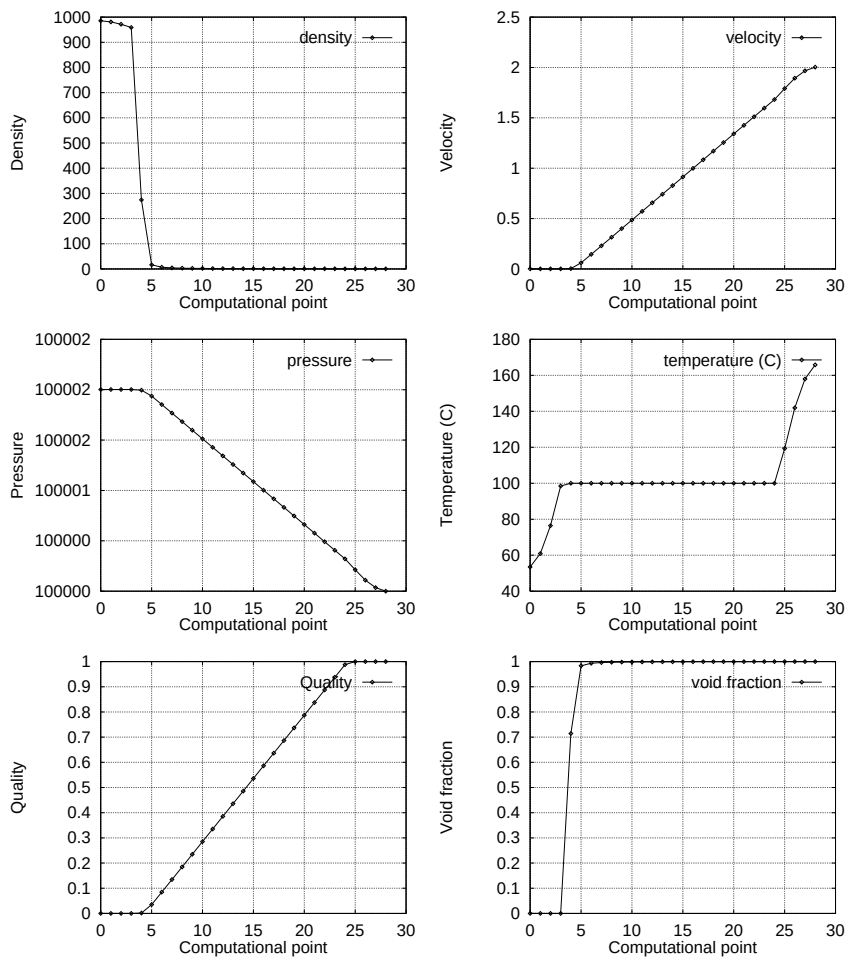

Figure 5: Profiles of steady solutions for the boiling water problem

7.2 Fall of pressure in a crack by friction

The problem consists in simulating the flow of water into a crack that connects two reservoirs. Such critical configurations can be encountered in tubes of vapour generators of nuclear power stations where the width of the cracks does not exceed 10 microns, but the critical mass flux (sonic flux) can reach 5 m^3h^{-1}. Generally, the engineers want to known the critical mass flux for a given shape of crack and generating pressure conditions in reservoirs. The critical mass flux corresponds to a maximum mass flux and is observed when a sonic point condition is reached at the crack outlet. This is the limit case of boundary conditions where one information comes back up from the outflow.
For our simulation, we suppose that the velocity field is homogeneous ($u_r = 0$) and that the section of the crack is constant, equal to 10^{-5} m. The friction at the crack lining induces the fall of pressure. It is represented by the term

$$S_2(v) \;=\; -k\sigma\rho u\,|u|,$$

where k is a friction constant. It also induces a source term on the energy equation $S_3(v) = S_2\,u$. The *Electricité de France* subdivision department DER/RNE/TTA has realized an experimental test bed for crack flows. It has been concluded that the effects of metastable saturated liquid could not be neglected if we want to get realistic simulations (see Pagès and Lebonhomme [38]). That is why we here enrich our model by adding two equations. The first one expresses the evolution of the fraction X, $0 \leq X \leq 1$ of liquid which is metastable. The source term expresses the relaxation to the saturated liquid. Written in conservation form, this gives

$$\frac{\partial}{\partial t}\left(\rho\sigma X\right) + \frac{\partial}{\partial x}\left(\rho u\sigma X\right) \;=\; -\;\frac{\sigma\rho X}{\Delta t_{rel}}, \tag{32}$$

where the characteristic time of relaxation Δt_{rel} has to be designed. The second equation expresses the isentropic evolution of the metastable liquid at entropy $s_{l;met}$:

$$\frac{\partial}{\partial t}\left(\rho\sigma s_{l;met}\right) + \frac{\partial}{\partial x}\left(\rho u\sigma s_{l;met}\right) \;=\; 0. \tag{33}$$

This five equation conservation system has to be closed. A metastable liquid can be associated to a metastable temperature T_{met} which is a function of the entropy $s_{l;met}$ and pressure p. From section 4, we deduce the law

$$T_{met} \;=\; T_{met}(p, s_{l;met}) \;=\; T_0 \exp\left(\frac{s_{l;met} - s_l^0 - \eta(p - p_0)}{c_l^0}\right).$$

We also define both metastable specific volume and enthalpy by

$$\tau_{l;met}(p, s_{l;met}) \;=\; \tau_l(p, T_{met}(p, s_{l;met})), \quad h_{l;met}(p, s_{l;met}) \;=\; h_l(p, T_{met}(p, s_{l;met})).$$

Specific volume and enthalpy for the mixture are

$$\begin{aligned}
\tau \;&=\; \tau(C, p, X, s_{l;met}) \;=\; C\tau_{v;sat}(p) + (1 - C - X)\tau_{l;sat}(p) + X\tau_{l;met}(p, s_{l;met}),\\
h \;&=\; h(C, p, X, s_{l;met}) \;=\; Ch_{v;sat}(p) + (1 - C - X)h_{l;sat}(p) + Xh_{l;met}(p, s_{l;met}),
\end{aligned}$$

where $\tau_{v;sat}(p) = \tau_v(p, T_{sat}(p))$ and $\tau_{l;sat}(p) = \tau_l(p, T_{sat}(p))$. In one-phase flows, we use the same model as presented for the injector-condenser.

For the simulation, we use 29 computational points. The crack length L is equal to 7. We have used the following function of friction coefficient:

$$\begin{aligned} k(x,t) &= k_{max}\ x\ r(t) \text{ if } x < 1\,, \\ &= k_{max}\ r(t) \text{ if } 1 \leq x < 5\,, \\ &= k_{max}\,(1-(x-5)))\ r(t) \text{ if } 5 \leq x < 6\,, \\ &= 0 \text{ if } 6 \leq x \leq 7\,, \end{aligned}$$

where $k_{max} = 3\,500\,000$ and $r(t) = \min\left(1, \frac{t}{2.5}\right)$. We still have to model the characteristic time $\Delta t_{t;rel}$. In this validation stage, we only use a term that ensures the fall of X to zero at the end of the computational domain, namely

$$\Delta t_{rel}(x) \;=\; \frac{1}{2}\ \max\left(\frac{L-x}{\sqrt{u^2+\epsilon^2}}, \frac{\Delta x}{\sqrt{u^2+\epsilon^2}}\right),$$

where ϵ is a small parameter, here chosen equal to 10^{-2}. For a more realistic relaxation model, see for example the discussion in [38]. At the entrance, we impose $\rho u = 10$ and h compatible with a pure liquid at temperature $T = 99.5$ C. When the first bubbles appear, we suppose that the liquid phase is almost completely metastable, with $X = 0.999$ and metastable temperature $T_m = T$. Outlet boundary conditions are $p = 50\,000$ Pa. The initial flow is liquid, uniform with data $\rho u = 10$, $p = 1$ bar, $X = 0.999$ and $T_m = T = 99.5$ C. On figure 6 the numerical solutions are presented after convergence to the steady flow. The thermodynamic quantities evolve correctly. Boiling conditions are reached; the variable C increases up to 0.0318 at the outlet. One can observe the brutal acceleration of the fluid at the end of the computational domain due to the quadratic nature of the friction source term. The problem is difficult to solve because of large characteristic time ratios between convection and return to local equilibrium. Thus, CFL numbers could not exceed the value of 5 during the computation. At the outlet boundary condition, the sonic point conditions are not reached yet because of difficulties encountered with this problem. The slope on pressure profile should tend to $-\infty$ at sonic conditions, which is not reached here but the numerical profile is not so far from a such singular behaviour. We are still working on the critical mass flux and the treatment of sonic boundary conditions.

8 Conclusion and future work

In this paper, we have shown the capacity of the Characteristic Flux Method to capture two-phase flows. In our opinion, the example of the HEM model is not restrictive and the method could be extended to finer models like those with six equations. We set a general numerical test bed with a very adaptive and modular code written in C++. A large part of this code is independent of both model and equations which can enable to compare different models. We have also presented a procedure to set very simple equations of state (EOS) that

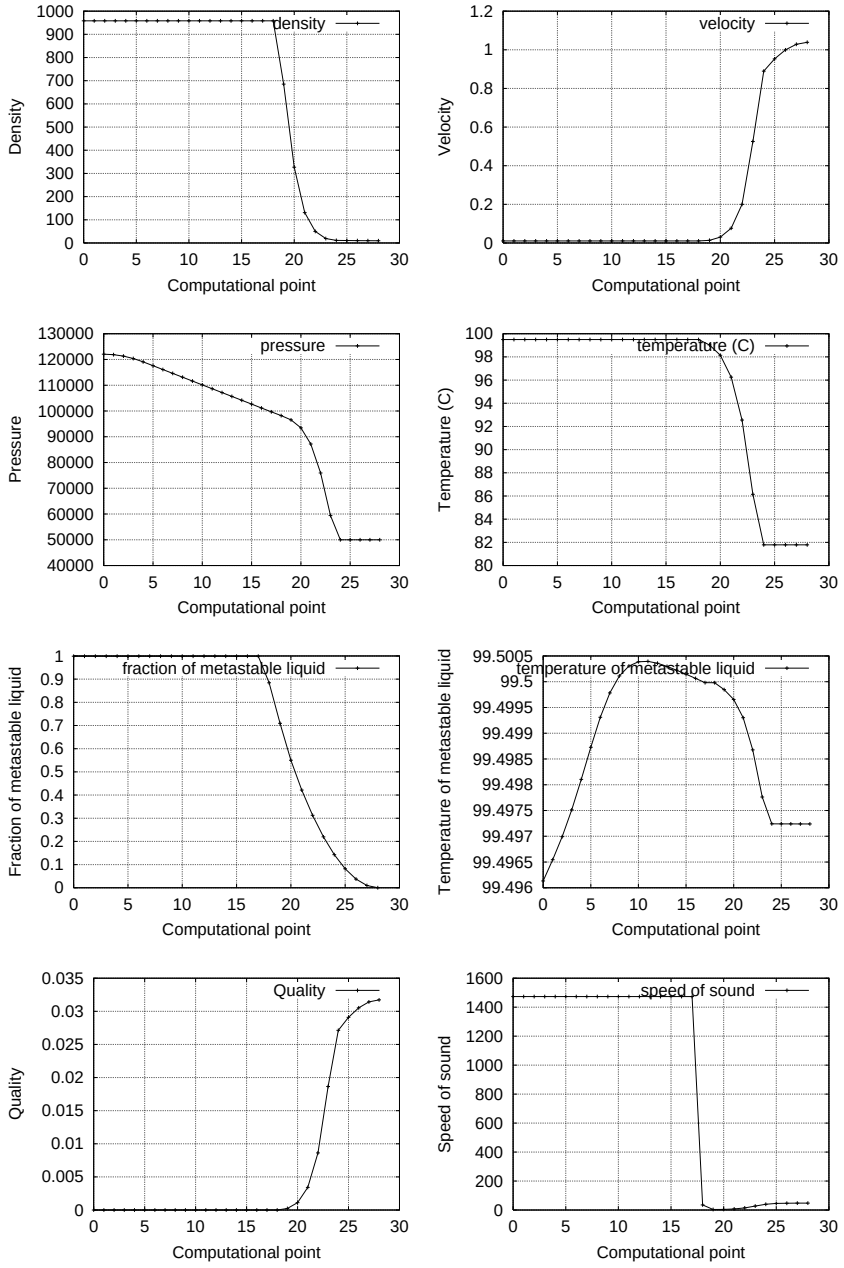

Figure 6: Profiles of steady solutions for the problem of fall in pressure using ECREVISSE model

accelerate the computation. Of course, it is not so accurate as if we used spline-based water tabulated laws, but this is sufficient for us to reproduce the water behaviour and make appear difficulties of two-phase flows. This can be viewed here as a trick to get faster computations, but of course water tables can be used.

The simulations of one-dimensional flows in channels of variable cross section have shown the capacity of the method to deal with regions of strong gradient of density, but also with free boundary phase transition and possibly appearing/desapearring phase. But it still reveals a lack of robustness at phase transitions which has not been completely understood yet. One of our interpretation is the following one: it would seem that the fully nonlinear implicit method is multivaluated (and thus not well-posed); this feature seems to be more sensible when discontinuities on Jacobian matrices are present.
The current research is aimed at achieving a variant of the Flux Scheme method that is entropy satisfying and that takes into account the phase transition feature intrinsically in its script.

Acknowledgments

The present work was done in the framework of a collaboration between *Electricité de France DR&D, Département Mécanique des Fluides et Transferts Thermiques* and the *Centre de Mathématiques et de Leurs Applications, ENS Cachan-CNRS*, France.

9 Appendix A : Derivation of the Homogeneous Equilibrium Model

In this Appendix, our aim is to describe how the Homogeneous Equilibrium Model can be derived from a 6 equation two-fluid model. In the setting of the so-called averaged model (see *e.g.* ISHII [32]), the description of the flow of a diphasic mixture is given in terms of phasic variables. In the case of a quasi-1D flow, the evolution equations describing the balances of mass, momentum and total energy read as follows :

$$\frac{\partial \alpha_v \rho_v \sigma(x)}{\partial t} + \frac{\partial \alpha_v \rho_v u_v \sigma(x)}{\partial x} = \sigma(x)\Gamma_{l\to v}\,, \tag{34}$$

$$\frac{\partial \alpha_\ell \rho_\ell \sigma(x)}{\partial t} + \frac{\partial \alpha_\ell \rho_\ell u_\ell \sigma(x)}{\partial x} = \sigma(x)\Gamma_{v\to l}\,, \tag{35}$$

$$\frac{\partial \alpha_v \rho_v u_v \sigma(x)}{\partial t} + \frac{\partial (\rho_v u_v^2 + p)\alpha_v \sigma(x)}{\partial x} = p\frac{\partial \alpha_v \sigma(x)}{\partial x} + \sigma(x)(f_{l\to v} + \Gamma_{l\to v} u_{l,v})\,, \tag{36}$$

$$\frac{\partial \alpha_\ell \rho_\ell u_\ell \sigma(x)}{\partial t} + \frac{\partial (\rho_\ell u_\ell^2 + p)\alpha_\ell \sigma(x)}{\partial x} = p\frac{\partial \alpha_\ell \sigma(x)}{\partial x} + \sigma(x)(f_{v\to l} + \Gamma_{v\to l} u_{v,l})\,, \tag{37}$$

$$\frac{\partial \alpha_v \rho_v (e_v + u_v^2/2)\sigma(x)}{\partial t} + \frac{\partial \rho_v u_v (e_v + p/\rho_v + u_v^2/2)\alpha_v \sigma(x)}{\partial x} = \\ = -p\frac{\partial \alpha_v \sigma(x)}{\partial t} + \sigma(x) Q_{l\to v}\,, \tag{38}$$

$$\frac{\partial \alpha_\ell \rho_\ell (e_\ell + u_\ell^2/2)\sigma(x)}{\partial t} + \frac{\partial \rho_\ell u_\ell (e_\ell + p/\rho_\ell + u_\ell^2/2)\alpha_\ell \sigma(x)}{\partial x} = \\ = -p\frac{\partial \alpha_\ell \sigma(x)}{\partial t} + \sigma(x) Q_{v\to l}\,. \tag{39}$$

Let us now describe the physical meaning of each variables : α_i is the volume fraction of the fluid i, ρ_i is the density of the fluid i, u_i denotes the velocity of the phase i and p is the thermodynamic pressure. Denoting by e_i the specific internal energy of the phase i, we have set $E_i = e_i + \frac{1}{2}|u|^2$: the total specific energy of the fluid i and $H_i = E_i + \frac{p}{\rho_i}$ the total specific enthalpy of the fluid i (we shall also use the notation $h_i \equiv e_i + \frac{p}{\rho_i}$ for the specific enthalpy of the fluid i).

We have the relation $\alpha_v + \alpha_\ell = 1$ and in order to close the system (34) to (39), we have to write two equations of state :

$$F_i(p, \rho_i, e_i) = 0\,, i = 1, 2\,. \tag{40}$$

The right hand sides of equations (34), (35) contain mass transfer terms $\Gamma_{v\to\ell}$ and $\Gamma_{\ell\to v}$ which satisfies $\Gamma_{v\to\ell} + \Gamma_{\ell\to v} = 0$. Similarly, equations (36), (37) contain momentum transfer

terms $f_{\ell\to v} + \Gamma_{\ell\to v} u_{\ell,v}$ and $f_{v\to\ell} + \Gamma_{\ell\to v} u_{\ell,v}$ with $f_{\ell\to v} + f_{v\to\ell} = 0$. Finally, equations (38), (39) contain momentum transfer terms $Q_{v\to\ell}$ et $Q_{\ell\to v}$ with $Q_{v\to\ell} + Q_{\ell\to v} = 0$.
Introducing the mean variables : $\rho = \alpha_v\rho_v + \alpha_\ell\rho_\ell$, $\rho u = \alpha_v\rho_v u_v + \alpha_\ell\rho_\ell u_\ell$, $\rho E = \alpha_v\rho_v E_v + \alpha_\ell\rho_\ell E_\ell$, and the concentration $C \equiv \alpha_v\rho_v/\rho$ together with the relative velocity $u_r \equiv u_v - u_\ell$, we obtain equations (1) to (3) by simply adding two by two the phasic equations, once the total energy is defined by (4) and the latent heat by $L \equiv h_v - h_\ell$.

10 Appendix B : The approximate problem from Homogeneous Equilibrium model

we should stress on whether the system (1) to (3) is its hyperbolic or not. Since this property is independent of σ, we take $\sigma \equiv 1$). This question is more simply investigated with the following quasilinear formulation :

$$\rho_t + (\rho u)_x = 0, \tag{41}$$

$$u_t + uu_x + \frac{1}{\rho}(p + C(1-C)u_r^2)_x = 0\,, \tag{42}$$

$$s_t + us_x + \frac{1}{\rho}(\rho C(1-C)\frac{L}{T}u_r)_x = 0\,, \tag{43}$$

where the specific entropy function s is defined thanks to the two first laws of thermodynamics ($\tau \equiv 1/\rho$) :

$$Tds = de + pd\tau\,. \tag{44}$$

Proposition 7 *We assume that the slip velocity u_r is a given constant. Denoting by Π and Φ the two functions of the 2 independent variables ρ and s, $\Pi \equiv p + C(1-C)u_r^2$ and $\Psi \equiv \rho C(1-C)\frac{L}{T}u_r$, the system (41) to (43) will have real characteristics if and only if*

$$\Delta \equiv 36\left(\frac{\partial\Pi}{\partial\rho}\right)^3\rho^4 - 72\left(\frac{\partial\Pi}{\partial\rho}\right)^2\rho^2\left(\frac{\partial\Psi}{\partial s}\right)^2 + 36\left(\frac{\partial\Pi}{\partial\rho}\right)\left(\frac{\partial\Psi}{\partial s}\right)^4 + 324\left(\frac{\partial\Psi}{\partial s}\right)\left(\frac{\partial\Pi}{\partial\rho}\right)\rho^2\left(\frac{\partial\Psi}{\partial\rho}\right)\frac{\partial\Pi}{\partial s} - 36\left(\frac{\partial\Psi}{\partial s}\right)^3\left(\frac{\partial\Psi}{\partial\rho}\right)\frac{\partial\Pi}{\partial s} - 243\,\rho^2\left(\frac{\partial\Psi}{\partial\rho}\right)^2\left(\frac{\partial\Pi}{\partial s}\right)^2 \geq 0\,. \tag{45}$$

Moreover when $\Delta > 0$, the three roots are distinct.

Proof. We linearize system (41) to (43) around a constant state (ρ, u, s) and look for nonvanishing plane wave solutions $Ve^{i(kx-\omega t)}$. Real characteristics will correspond to the case where the only possible solutions occur for k and ω real. This amounts to saying that the roots of the characteristic polynomial are real. This polynomial is here

$$\lambda^3 + \frac{1}{\rho}\frac{\partial\Psi}{\partial s}\lambda^2 - \frac{\partial\Pi}{\partial\rho}\lambda + \frac{1}{\rho}\left(\frac{\partial\Psi}{\partial\rho}\frac{\partial\Pi}{\partial s} - \frac{\partial\Pi}{\partial\rho}\frac{\partial\Psi}{\partial s}\right), \tag{46}$$

and the result follows by simply computing its discriminant.

Remark 1 *In the case where $u_r \equiv 0$, as expected, condition (45) reads as* $\left(\frac{\partial p}{\partial \rho}\right)_s \geq 0$.

11 Appendix C : equation of state, respect of the first principle of Thermodynamics and entropies

Let first consider the one-phase fluid case (pure liquid or dry vapour). The first principle of Thermodynamics stipulates that

$$\frac{1}{T}\, de \;+\; \frac{p}{T}\, d\tau$$

is the total differential of a function, see (44). Since $h = e + p\tau$, we can also write

$$ds = \frac{1}{T}\, dh - \frac{\tau}{T}\, dp. \tag{47}$$

The compatibility relation on the crossed partial derivatives leads to the two first constraints

$$\left(\frac{\partial h}{\partial p}\right)_T \;=\; -T^2 \left(\frac{\partial}{\partial T}\left(\frac{\tau}{T}\right)\right)_p \tag{48}$$

for both the liquid and the vapour phases. Once expression (48) holds true, the expression of the entropy s_k of each phase ($k = v$ or l) is then deduced from (47) by integrating.

Let us consider now the mixture case. To express the first principle of Thermodynamics in that case, it is convenient to introduce the latent heat L defined as the difference of enthalpies between the two phases in the saturated mixture

$$L(T) = h_{v;s}(T) - h_{l;s}(T). \tag{49}$$

If we express the differential function of the enthalpy function of L and C

$$dh = \left(C\,\frac{dL}{dp} + \frac{dh_\ell}{dp}\right) dp + L\, dC, \tag{50}$$

and inject it in (47), this shows that

$$\frac{L}{T}\, dC + \frac{c\frac{dL}{dp} - \tau + \frac{dh_\ell}{dp}}{T}\, dp$$

is a total differential. It is true if and only if

$$\frac{\partial}{\partial p}\left(\frac{L}{T}\right) = \frac{\partial}{\partial C}\left(\frac{C\frac{dL}{dp} + \frac{dh_\ell}{dp} - \tau}{T}\right). \tag{51}$$

This third constraint is written quite simply as

$$L\frac{dT}{dp} = T(\tau_v - \tau_\ell)\,. \tag{52}$$

This is the famous Clapeyron's law. The entropy law of the mixture can be deduced by integrating (52) :

$$s = \frac{C\,L}{T} - \int_{p_0}^{p} \frac{\tau_\ell - \frac{dh_\ell}{dp}}{T} dp\,. \tag{53}$$

Let us now denote by c_v the mass heat of saturated vapour and by c_ℓ the heat mass of saturated liquid. We then have by definition of the c_k's

$$T ds_k = c_k\, dT \text{ for } k \in \{v, l\}\,. \tag{54}$$

This can be rewritten, using (47), as

$$c_k = \left(\frac{dh_k}{dT} - \tau_k \frac{dp_s}{dT} \right)\,. \tag{55}$$

Thus, coupling with Clapeyron's law (52), we have

$$c_v - c_\ell = \frac{dL}{dT} - \frac{L}{T}\,, \tag{56}$$

and

$$\tau_\ell - \frac{dh_\ell}{dp} = -c_\ell \frac{dT}{dp}\,, \tag{57}$$

$$s \;=\; \frac{c\,L}{T} + \int_{T_0}^{T} \frac{c_\ell}{T} dT\,. \tag{58}$$

In our context of water flow, it is reasonable to suppose that when c_ℓ is constant, then 58 becomes

$$s \;=\; \frac{cL}{T} + c_\ell^0 \log \frac{T}{T_0}\,. \tag{59}$$

First reduction

Lemma 1 *Suppose that the law $\tau_v(p,T)$ is of the form*

$$\tau_v(p,T) \;=\; T\;\kappa(p) \tag{60}$$

for a given function κ. In addition to this, let's suppose more that τ_ℓ has the form

$$\tau_\ell(p,T) \;=\; \varphi_1(p) \;+\; \varphi_2(T). \tag{61}$$

and that the function

$$h_\ell(p_0,T) \;=\; \varphi(T) \tag{62}$$

is a known function at a given pressure p_0. Then the specific enthalpy of the vapour h_v is a function Ψ of the only temperature and h_ℓ and Ψ are given by

$$h_\ell(p,T) \;=\; \varphi(T) + \int_{p_0}^{p} \varphi_1(q)dq + \left(\varphi_2(T) - T\varphi_2'(T)\right)(p - p_0) \tag{63}$$

$$\begin{aligned} \Psi(T) \;=\; & \varphi(T) + \int_{p_0}^{p_s(T)} \varphi_1(q)dq - T^2\left(\varphi_2(T)/T\right)'(T)\,(p_s(T) - p_0) \\ & + Tp_s'(T)\;\left(T\kappa(p_s(T)) - \varphi_1(p_s(T) - \varphi_2(T)\right). \end{aligned} \tag{64}$$

The liquid, vapour and mixture entropies are given by

$$s_\ell(p,T) = s_\ell^0 + \int_{T_0}^{T} \frac{\varphi'(t)}{t} dt - \varphi_2'(T)(p-p_0) - [\varphi_2'(T) - \varphi_2'(T_0)](p-p_0), \tag{65}$$

$$s_v(p,T) = s_v^0 + \int_{T_0}^{T} \frac{\Psi'(t)}{t} dt - [\lambda(p) - \lambda(p_0)], \tag{66}$$

$$s(C,T) = C s_{v;s}(T) + (1-C) s_{l;s}(T) \tag{67}$$

$$= s_0 + \frac{CL}{T} + \int_{T_c}^{T} \left[\frac{\varphi'(t)}{t} - \varphi_2''(t)(p_s(t) - p_c) - \varphi_2'(t) p_s'(t) \right] dt.$$

Proof. The fact that $\tau_v = \Psi(T)$ is an immediate consequence of (48) under (60). Expression (63) is obtained on an integration of 48 for the liquid phase using (62). Expression (64) is only Clapeyron's law (52) under the hypotheses of the lemma.

We see that we have five real unknown functions $p_s(T)$, κ, $\varphi(T)$, $\varphi_1(p)$ and $\varphi_2(T)$. If the primitive of φ_1 is known, then the laws on h_ℓ and h_v become explicit using expressions (63) and (64).

Second reduction : choice for the pressure of saturation

Lemma 2 *Let us keep the hypotheses of lemma 1 and denote by λ a primitive function of κ. If $p_s(T)$ is the solution of the differential equation*

$$\frac{d}{dT}\left[\lambda(p_s(T))\right] = \frac{L_0}{T^2} \tag{68}$$

for a given constant L_0, then

$$\Psi(T) = h_{l;s}(T) + L_0 \left(1 - \frac{\tau_{l;s}(T)}{\tau_{v;s(T)}} \right). \tag{69}$$

Remark 2 *Lemma 2 shows that, under the additional hypothesis (68) and because $\tau_{l;s} << \tau_{v;s}$ in the case of water, the specific vapour enthalpy is almost a constant L_0. This approximation is reasonable for the water. So it is also normal to calibrate L_0 as the latent heat for given conditions of saturation. The remaining unknown functions are then φ, φ_1, φ_2 and κ.*

Remark 3 *The differential equation (68) is just Clapeyron's law, altered with the following approximations : the latent heat is approximated by a constant L_0, $\tau_{v;s} - \tau_{l;s}$ is approximated by $\tau_{v;s}$, and τ_v has the form (60). Under these assumptions, we have*

$$L_0 \frac{dT_s}{dp} = T\tau_{v;s} = T^2 \kappa(p_s)$$

so that

$$\frac{L_0}{T^2} = p_s'(T)\kappa(p) = \frac{d\lambda(p_s(T))}{dT}.$$

11.1 Examples of partly linear or parabolic laws of state

To close the formulae, we decide to use either a linear or a quadratic function for φ_1, φ_2 or φ and a "simple" function κ.

Proposition 8 *Let us choose*

$$\kappa(p) = \frac{R}{p}, \tag{70}$$

$$\tau_\ell(p,T) = \tau_\ell^0 + \xi(p-p_0) + \eta\,(T-T_0) + \frac{\nu}{2}(T-T_0)^2\,, \tag{71}$$

$$\varphi(T) = h_\ell^0 + c_\ell^0(T-T_0). \tag{72}$$

$$\tag{73}$$

Then, it comes

$$p_s(T) = p_c\ \exp\left[\frac{L_0}{R}\left(\frac{1}{T_c}-\frac{1}{T}\right)\right]. \tag{74}$$

$$\begin{aligned} h_\ell(p,T) &= h_\ell^0 + c_\ell^0(T-T_0) - \nu(T^2-T_0^2)p + (\tau_\ell^0 - \eta T_0)(p-p_0) \\ &\quad + \frac{\xi}{2}(p-p_0)^2\,, \end{aligned} \tag{75}$$

$$h_v(T) = \psi(T) = h_\ell(p_s(T),T) + L_0\left(1-\frac{\tau_{ls}(T)}{\tau_{vs}(T)}\right), \tag{76}$$

$$\tag{77}$$

with entropies

$$\begin{aligned} s_\ell(p,T) &= s_\ell^0 - [\eta + 2\nu(T-T_0)](p-p_0) + c_\ell^0 \log\frac{T}{T_0}\,, \\ s_v(p,T) &= s_v^0 - R\log\frac{p}{p_0} + \int_{T_0}^{T}\frac{\psi'(t)}{t}dt\,, \\ s(C,T) &= s_0 + \frac{C\,L}{T} - [\eta + \nu(T-T_0)](p_s(T)-p_c) + c_\ell^0\log\frac{T}{T_c}\,. \end{aligned}$$

11.2 Computation of constants of the model using water tables

We now have to end up with the equations of state by providing physical values for all these constants. This is reached by using the tables of water. We first choose a range of variation for the pressure and temperature. Then we choose constant states $(\tau(p_0,T_0), h(p_0,T_0))$ and deduce from the table derivates quantities such as $\frac{\partial\tau}{\partial p}_{|T=T_0}$ or $\frac{\partial\tau}{\partial T}_{|p=p_0}$. The values presented on tables 1 and 2 are obtained for a pressure respectively close to 1 bar and 6 bar, and for a temperature close to the saturation conditions. Finally, on figure 7 we compare these analytical equations of state with constants of Table 1, to real data extracted from VDI water tables. We do observe that our laws thoroughly match the VDI tables for a pressure

ξ	$-5.36e-13$	L_0	$2300e3$
η	$6.22e-7$	R	456.31
p_0	$1.1e5$	τ_ℓ^0	$1.0438e-3$
T_0	373.15	h_ℓ^0	$418.9e3$
p_c	$1.013e5$	c_ℓ^0	$4194.$
T_c	373.15		

Table 1: Table of constants used for a range of pressure or order 1 bar

ξ	$-6.40e-13$	L_0	$2085.08e3$
η	$7.843e-7$	R	443.032
p_0	$6.0e5$	τ_ℓ^0	$1.0698e-3$
T_0	403.15	h_ℓ^0	$546.525e3$
p_c	$6.e5$	c_ℓ^0	$4200.$
T_c	432.0		

Table 2: Table of constants used for a range of pressure or order 6 bar

in a range from 0.5 bar to 6 bar and for a temperature near saturation conditions. Errors on vapor specific enthalpy profiles are more noticeable because of the lack of freedom on these laws due to the constraint for respecting the entropy. One can notice a relative error of about 3 percent on enthalpy near 1 bar. But this is sufficient to validate numerical methods, or to compute intermediate results before applying more accurate tabulated laws for example.

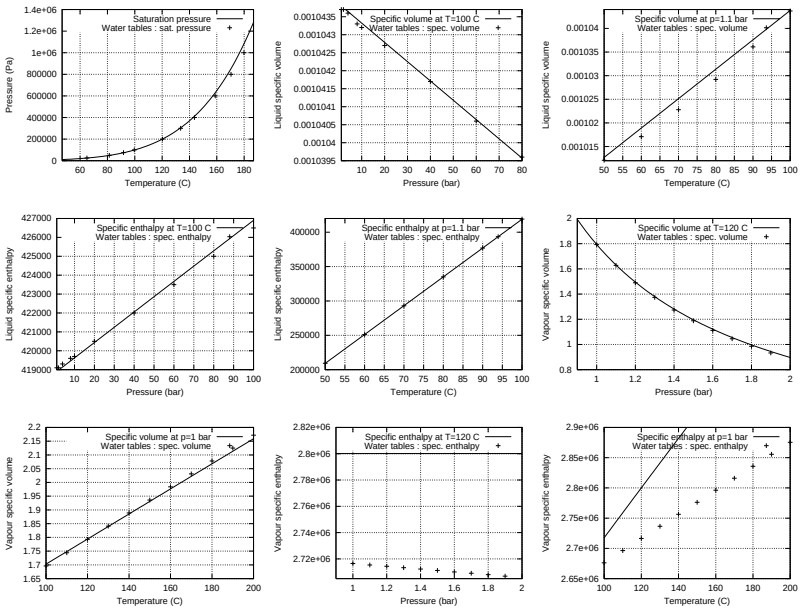

Figure 7: Comparison between analytical equations of state and water tables: saturation pressure, liquid and vapor specific volume and enthalpy. Model constants available in the vicinity of $p = 1$ *bar* and saturation conditions

References

[1] ALOUGES F., GHIDAGLIA J.-M. and TAJCHMAN M., On the interaction of upwinding and forcing for nonlinear hyperbolic systems of conservation laws, Publication du CMLA nb 9907, ENS Cachan, 1999.

[2] BESTION D., The physical closure laws in the CATHARE code, Nucl. Eng. Design, 124, 229-245, 1990.

[3] BESTION D., The phase apprearance et disappearance in the CATHARE code, CEA Report, SMTH/MLDS/200-061, 2000.

[4] BOURE J.A. and DELHAYE J.-M., General Equations and Two-Phase Flow Modeling, in *Handbook of Multiphase Systems*, G. Hestroni, Ed., Hemisphere, 1982.

[5] BOUCKER M., *Modélisation numérique multidimensionnelle d'écoulements diphasiques liquide-gaz en régimes transitoires et permanents : méthodes et applications*, Thèse, ENS-Cachan, France, 1998.

[6] BOUCHUT F., Entropy satisfying flux vector splittings and kinetic BGK models, Numer. Math., 94(1), 623–672, 2003.

[7] COCCHI J.P. and SAUREL R., A Riemann Problem Based Method for Compressible Multifluid Flows, J. Comput. Phys., 137, 265-298, 1987.

[8] COQUEL F., EL AMINE K., GODLEWSKI E., PERTHAME B. and RASCLE P., A Numerical Method Using Upwind Schemes for the Resolution of Two-Phase Flows, J. Comput. Phys., 136, 272-288, 1997.

[9] COQUEL F. and LIOU M.S., *Hybrid upwind splitting (HUS) by a field-by-field decomposition*, NASA TM-106843, Icomp-95-2 (1995).

[10] COQUEL F. and PERTHAME B., Relaxation of energy and approximate Riemann solvers for general pressure law in fluid dynamics, SIAM J. Numer Anal. 35(6) 2223-2249 (1998)

[11] DEBERNE N., Modélisation et expérimentation des Injecteurs-condenseurs, PhD Thesis, INSA Lyon France (2000).

[12] DECLERCQ E. , FORESTIER A., HERARD J. M., LOUIS X. and POISSANT G., "An exact Riemann solver for a multicomponent turbulent compressible flow". Int. J. of Comp. Fluid Dynamics, vol.14, pp. 117-131 (2001).

[13] DE VUYST F., Construction de schémas de flux s'appuyant sur une formulation cinétique champ par champ, C. R. Acad. Sci. Série I, vol. 330(4), pp. 321-326 (2000)

[14] DE VUYST F. *et al*, Numerical modeling of two-phase water flows using flux schemes. application to the injector-condenser and boiling water in a hot channel, groupe de travail sur les schémas de flux, IESC Cargèse, 22-24 septembre 1999, electronic editions *http://www.cmla.ens-cachan.fr/Utilisateurs/perfortmans/*

[15] DE VUYST F., GHIDAGLIA J.-M. and LE COQ G., Partly linearized laws of state for modeling two-phase flows and numerical computation using flux schemes, AMIF-ESF Worshop "Computing methods for two-phase flow", Aussois, France, Jannuary 2000.

[16] DE VUYST F., GHIDAGLIA J.M., LE COQ G., Mimouni S., Pagès D., Partly linearized laws of state for modeling two-phase flow and numerical computation using flux schemes, Séminaire DRN/MFN, CEA Saclay, France, 24-26 janvier 2000.

[17] DREW D.A. and LAHEY R.T., Application of General Constitutive Principles to the Derivation of Multidimensional Two-Phase Flow Equations, Int. J. Multiphase Flow, 5, 243-264, 1979.

[18] DREW D.A. and WALLIS G.B., Fundamentals of Two-Phase Flow Modeling, in *Multiphase Science and Technology, Volume 8*, Hewitt *al* Editors, Begell House, Inc., New-York, 1994.

[19] FAILLE I. and HEINTZE., A Rough Finite Volume Scheme for Modeling Two-Phase Flow in a Pipeline, Computers & Fluids, 28, No. 2, p. 213-241, 1999.

[20] GHIDAGLIA J.-M., *Une approche volumes finis pour la résolution des systèmes hyperboliques de lois de conservation*,Note, Département Transferts Thermiques et Aérodynamique, Direction des Etudes et Recherches, Electricité de France, HT-30/95/015/A, 1995.

[21] GHIDAGLIA J.-M., Flux schemes for solving nonlinear systems of conservation laws, *Proceedings of the meeting in honor of P.L. Roe*, Chattot J.J. and Hafez M. Eds, Arcachon, July 1998.

[22] GHIDAGLIA J.-M., KUMBARO A. and LE COQ G., Une méthode volumes-finis à flux caractéristiques pour la résolution numérique des systèmes hyperboliques de lois de conservation, *C.R.Acad. Sc. Paris*, 1996, **322**, I, 981-988.

[23] GHIDAGLIA J.-M., KUMBARO A. and LE COQ G., On the numerical solution to two fluid models *via* a cell centered finite volume method, Europ. Journal Mech. B/Fluids, 20, 841–867, 2001.

[24] GHIDAGLIA J.-M., KUMBARO A., LE COQ and TAJCHMAN M., A finite volume implicit method based on characteristic flux for solving hyperbolic systems of conservation laws, *Proceedings of the Conference on : Nonlinear evolution equations and infinite-dimensional dynamical systems* (Shanga June 1995), Li Ta-Tsien Ed., 1997, World Scientific, Singapore.

[25] GHIDAGLIA J.-M., LE COQ G. and TOUMI I., Two flux schemes for computing two phases flows throught multidimensional finite volume methods, Proceedings of the NURETH-9 conference, October 1999, San Francisco, American Nuclear Society.

[26] GUILLARD H. and MURONE, A., A five equation reduced model for compressible two pahse flow problems, INRIA Technical report RR-4778 (2003).

[27] GÖZ M.F. and MUNZ C.-D., Approximate Riemann Solvers for Fluid Flow with Material Interfaces, in *Numerical Methods for Wave Propagation*, E.F. Toro and J.F. Clarke, Eds., 211-235, Kluwer Academic Publishers, 1998.

[28] GUILLARD H., Mixed element volume methods in computational fluid Dunamics, *Lecture Series, Von Karman Institute for fluid Dynamics*, 1995.

[29] HALAOUA K., *Quelques solveurs pour les opérateurs de convection et leurs applications la mécanique des fluides diphasiques*, Thèse de doctorat, ENS-Cachan, France, 1998.

[30] HARTEN A., LAX P.D. and VAN LEER B., *On upstream differencing and Godunov-type schemes for hyperbolic conservation laws*, SIAM Review, 25 (1983), pp. 35-61.

[31] HEWITT G.F., DELHAYE and ZUBER M., *Numerical benchmark tests, in* Multiphase Science and Technology, vol. 3, Hemisphere, Washington DC/ New York, 1987.

[32] ISHII M., *Thermo-Fluid Dynamic Theory of Two-Phase Flow*, Eyrolles, Paris, 1975.

[33] KRÖNER D., *Numerical schemes for conservation laws*, Wiley Teubner, 1997.

[34] LIOU M.S., Low Mach Number and Two-Phase Flow Extensions of the AUSM Scheme, 30th VKI Computational Fluid Dynamics Lecture Series, 8-12 March, 1999.

[35] METRAL, J., Modélisation de l'écoulement de plasmas d'air hors-équilibre, Thesis of Ecole Centrale de paris, 2002.

[36] MIMOUNI S., BOUCKER M., LE COQ G. and GHIDAGLIA J.-M., *An overview of the VFFC-methods and tools for the simulation of two-phase flows*, Rapport EDF/DER/TTA/HT-33/99/006/A, Chatou, France, 1999.

[37] OSHER S. and SOLOMON F., "Upwind Difference Scheme for Hyperbolic Systems of Conservation Laws", Math. Comput., 38, 339-374, 1982.

[38] PAGES D. and LEBONHOMME S., Pagès D., Le Bonhomme S., *Logiciel ECREVISSE version 2.1, note de principe et notice utilisateur*, Note EDF HT-32/98/017/A, Châtou, 1998.

[39] RAMOS D., Existence and uniqueness for a mixed hyperbolic-parabolic problem, Proceedings of the workshop *Schémas de flux pour la simulation numérique des écoulements diphasiques*, Cargèse, France September 1999, http://www.cmla.ens-cachan.fr/Utilisateurs/perfortmans/ .

[40] RANSOM V.H., *Numerical Modeling of Two-Phase Flows*, Cours de l'Ecole d'été d'Analyse Numérique - CEA-INRIA-EDF, 12-23 juin 1989.

[41] RANSOM V.H. and HICKS D.L., Hyperbolic two-pressure models for two-phase flow revisited, J. Comput. Phys., 75, pp 498-504, 1988.

[42] ROE P.L., Approximate Riemann solvers, parameter vectors and difference schemes, J. Comput. Phys., 43, pp 357-372, 1981.

[43] ROMATE J.E., "Approximate Riemann Solvers for a Hyperbolic Two-Phase Flow Model", in Numerical Modelling in Continuum Mechanics, M. Feistauer, R. Rannacher and K. Kozel (Eds.), Proc. 3rd Summer Conference, Prague, 8-11 September, 1997.

[44] ROY M.F., Basic algorithms in real algebraic geometry and their complexity : from Sturm's theorem to the existential theory of reals, *Lectures in Real Geometry, Ed. : Fabrizio Broglia*, 1-67, Walter de Gruyter & Co., Berlin.

[45] RUSANOV V. V., Calculation of interaction of non-steady shock wave with obstacle, J. Comp. Math. Phys., USSR 1, 267-279 (1961).

[46] SAINSAULIEU L., Finite Volume Approximation of Two-Phase Fluid Flows Based on an Approximate Roe-type Riemann Solver, J. Comput. Phys., 121, 1-28, 1995.

[47] SAUREL R. and ABGRALL R., A Method for Compressible Multiphase Flows with Interfaces, Proc. ICMF'98, Third International Conference on Multi-Phase Flow, June 8-12, 1998, Lyon, France.

[48] SAUREL R. and LE METAYER O., A multiphase model for compressible flows with interfaces, shock, detonation wave and cavitation, Journal of Fluid Mechanics, 431, 239–273 (2001)

[49] STÄDTKE H. and HOLTBECKER R., Hyperbolic Model for Inhomogeneous Two-Phase Flow, Proc. Int. Conf. On Multiphase Flows, September 24-27, 1991, University of Tsukuba, Japan.

[50] STÄDTKE H., FRANCHELLO G. and WORTH B., Numerical Simulation of Multi-Dimensional Two-Phase Flow Based on Flux Vector Splitting, Nucl. Eng. Design, 177, 199-213, 1997.

[51] STEWART H.B., WENDROFF B., Two-phase flows : models and methods, *J. Comput. Phys.*, 1984, **56**, 363-409.

[52] TAJCHMAN M. and FREYDIER P., *Méthode Volumes Finis Flux Caractéristiques. Application un calcul bidimensionnel sur un maillage non conforme*, Note, Département Transferts Thermiques et Aérodynamique, Direction des Etudes et Recherches, Electricité de France, EDF HT-30/96/004/A, May 1996.

[53] TORO E.F., Riemann-Problem Based Techniques for Computing Reactive Two-Phase Flows, in *Numerical Combustion*, A. Dervieux and B. Larrouturou, Eds., Lect. Notes in Physics, 351, 472, Springer-Verlag, 1989.

[54] TOUMI I., A weak formulation of Roe's approximate Riemann solver , J. Comput. Phys. 102 (1992), 360-373.

[55] TOUMI I., An upwind numerical method for a six equation two-fluid model, Nuclear Science and Engineering, 123, 147-168 (1996).

[56] VAN LEER B., Flux Vector Splitting for the Euler Equations, ICASE Technical Report, No. 82-30, 1982.

[57] VAN LEER B., Towards the ultimate conservative difference scheme IV: a new approach to numerical convection, J. Comp. Phys. 23 (1977), pp; 276-279.